Evidence of a Tendency to Self-Association of the Transmembrane Domain of ErbB-2 in Fluid Phospholipid Bilayers†

Simon Sharpe, Kathryn R. Barber, and Chris W. M. Grant*

Department of Biochemistry, University of Western Ontario, London, Ontario, Canada N6A 5C1

Received June 26, 2001

ABSTRACT: The transmembrane domains of receptor tyrosine kinases are single-span helical structures suggested to participate directly in the formation of side-to-side receptor homodimers/homooligomers that modulate signal transduction. Transmembrane peptides from the class I receptor tyrosine kinase, ErbB-2, were examined directly by ^{2}H NMR spectroscopy as a means of following such phenomena under the dynamic conditions that characterize fluid, fully hydrated bilayers of natural phospholipids. Appropriate peptides were expressed as 50-mers, containing the transmembrane domain of ErbB-2 plus contiguous stretches of amino acids from the cytoplasmic and extracellular domains. Deuterium probes were incorporated in place of ^{1}H at a site within the helical intramembranous portion (the -CH_3 side chain of Ala^{657}), and the peptides were assembled into bilayers of 1-palmitoyl-2-oleoylphosphatidylcholine (POPC) for study. An analogous peptide corresponding to the oncogenic variant characterized by a Val^{659}→Glu point mutation was also examined. At high peptide concentration, prominent spectral features could be assigned to rapidly rotating transmembrane monomers and to large oligomers rotating very slowly relative to a time scale of 10^{-5} s. As peptide concentration was lowered, the latter feature was greatly reduced, and an additional population of mobile species became identifiable, consistent with the presence of homodimers and/or small oligomers. The defined nature of these latter spectral features suggests that preferred interaction sites exist on the peptides. The appearance of similar phenomena in the case of transmembrane peptides from both wild-type ErbB-2 and the transforming mutant argues for the involvement of additional factors in signal modulation, such as limitations normally imposed by the missing extramembranous portions.

Receptor spatial arrangement and associations are widely considered to be key determinants of signal transduction at the cell surface. Thus alterations that lead to receptor homodimer/homooligomer formation are often seen as activating steps in signal transmission. The receptor tyrosine kinases, which regulate growth and development, are prototypic examples of this reasoning, particularly the ErbB family in human cells (*1*, *2*). Overexpression of the ErbB family of receptors has been implicated in a wide range of human cancers and can correlate with poor prognosis, suggesting that high concentrations of these receptors in the membrane can overcome regulatory controls (*3*, *4*).

Receptor tyrosine kinases commonly consist of one polypeptide chain, containing an extracellular ligand-binding domain, a single-span helical transmembrane domain of 22−26 amino acids, and a cytoplasmic domain having kinase activity and recognition sites for cytoplasmic proteins (*1*, *3*, *5*, *6*). The concept has evolved that an important mechanism of homodimer formation for these receptors involves energetically favorable side-to-side association of their transmembrane portions. Sternberg and Gullick (*7*) have hypothesized that there is a dimerization motif within this region, suggesting that homodimer formation could occur via direct contact of the motifs in two neighboring receptors. The motif was originally described as being a five-residue segment in which the first amino acid has a small side chain, the fourth an aliphatic chain, and the fifth the smallest side chains only (Gly or Ala). Brandt-Rauf et al. (*8*) have emphasized the possible importance of transmembrane domain conformation in this side-to-side association. It has been noted that such concepts, alone or in combination, could account for the observation that certain point mutations within this sequence of five amino acids can induce abnormal cell behavior. A well-known example that has received structural attention is the substitution of valine by glutamate within the Sternberg−Gullick motif, which leads to transformed cell characteristics (*4*, *7*−*13*). Unfortunately the technical challenges of working with membrane proteins have made it difficult to directly test the models involved (*14*). Evidence of dimerization of transmembrane peptides from ErbB-2[1] (and the related Neu) has been observed on reducing SDS gels: separate bands can be seen corresponding to species of

† This research was supported by an operating grant to C.W.M.G. from the MRC of Canada. NMR spectroscopy was carried out in the McLaughlin Macromolecular Structure Facility, established with joint grants to the department from the R. S. McLaughlin Foundation, the London Life Insurance Co., the MRC Development Program, and the Academic Development Fund of UWO. S.S. is the holder of an NSERC PGSB scholarship.

* Corresponding author: Tel (519) 661-3065; fax (519) 661-3175; e-mail cgrant@uwo.ca.

10.1021/bi011340f CCC: $22.00
Published on Web 01/26/2002

monomer and dimer molecular weights (*9*, *15*). However it has been pointed out that significant differences can occur in transmembrane helix dimerization between detergent micelles and lipid bilayers (*15*−*17*). Smith has recorded apparent dimers/oligomers of Neu transmembrane peptides in dried phospholipid films and in gel-phase bilayers by magic-angle spinning (MAS) NMR (*11*) (see also ref *18*). In the present work, peptides containing the transmembrane domain of the class I receptor tyrosine kinase, ErbB-2, were studied in an effort to identify populations of species more complex than monomers within fluid fully hydrated bilayers of a common natural phospholipid.

Wide-line ^{2}H NMR is well suited to studying interactions among highly dynamic species in membranes. The spectra sensitively reflect orientation and behavior of deuterated molecules in a membrane environment. The technique has been well developed as it relates to transmembrane bacterial and model peptides (reviewed in refs *19*−*22*). However, there has been little use of wide-line ^{2}H NMR to study peptide−peptide interaction, a phenomenon of special interest to signaling in higher animal systems. In attempting to extend ^{2}H NMR to higher animal receptors, we have in the past described studies of transmembrane peptides from several receptor tyrosine kinases: the human EGF receptor (ErbB-1), rat Neu, and human ErbB-2 (*13*, *15*). Our previous efforts focused on spectral features associated with monomeric peptide. Here we examine spectral components reflecting behavior anticipated for peptides in homodimer/homo-oligomer states, in systems having peptide concentrations that might be considered to mimic receptor overexpression.

For purposes of NMR spectroscopy, alanine side chains were deuterated: i.e., alanine side chains were -CD_3 rather than -CH_3. This probe location is attractive since the methyl group of alanine is fixed directly to the peptide backbone, avoiding complexities arising from uncharacterized side-chain conformation or motion. Deuterated peptides were assembled into fluid bilayers of 1-palmitoyl-2-oleoylphosphatidylcholine (POPC), a common major phospholipid of cell membranes, and their spectra were examined over a range of temperature and peptide concentration. Spectra were also obtained for the peptides in POPC bilayers containing 33 mol % cholesterol, reflecting the sterol content of cell plasma membranes.

Since little information is available surrounding ^{2}H NMR effects of peptide side-to-side interactions, a similar expressed transmembrane peptide derived from ErbB-1 (the human EGF receptor) was examined. Past experience with this species is that its transmembrane domain displays a relatively limited tendency to self-associate (e.g., ref *15*).

[1] Abbreviations: ErbB-2, a human class I receptor tyrosine kinase also known as HER2 or c-erbB-2; EGF, epidermal growth factor; Neu, the rat homologue of ErbB-2; ErbB-2_{TM}, a 50-residue expressed transmembrane peptide containing Ser^{649} to Met^{691} of ErbB-2 plus Gly at position 648 and an N-terminal hexaHis tag; ErbB-2_{TM}Mu, the same peptide as the transmembrane peptide of ErbB-2 but containing the oncogenic Val^{657}→Glu mutation; ErbB-1_{TM}, a 38-residue expressed transmembrane peptide containing Pro^{620} to Arg^{651} of the human EGF receptor plus an N-terminal hexaHis tag; POPC, 1-palmitoyl-2-oleoylphosphatidylcholine; FACT, formic acid/acetic acid/chloroform/trifluoroethanol (1:1:2:1 ratio by volume).

EXPERIMENTAL PROCEDURES

Materials. 1-Palmitoyl-2-oleoyl-3-*sn*-phosphatidylcholine (POPC) and cholesterol were obtained from Avanti Polar Lipids (Birmingham, AL) and Sigma (St. Louis, MO), respectively. Deuterium-depleted water and deuteriomethyl L-alanine were from Cambridge Isotope Laboratories (Andover, MA). 2,2,2-Trifluoroethanol, NMR grade, bp 77−80 °C, was from Aldrich (Milwaukee, MI). Deuterated peptides were expressed by general procedures described previously (*13*, *15*). Briefly, His-tagged peptides were produced as TrpE fusion proteins, released from TrpE by cyanogen bromide cleavage, and purified by nickel-chelate chromatography (Ni−NTA resin, Qiagen GmbH). Peptide purification was monitored by SDS−polyacrylamide gel electrophoresis and confirmed by electrospray mass spectrometry. Site-directed mutagenesis [Promega Gene Editor in vitro system (Madison, WI)] was used to replace Ala^{648} in the native ErbB-2 sequence with Gly.

Preparation of Samples and NMR Spectroscopy. Liposome generation was according to the following protocol. The mixed organic solvent FACT (*13*) was used to prepare solutions of lipid plus peptide that could be dried to form thin films for subsequent hydration with sample buffer. Typically, dry peptide (10 mg) and appropriate amounts of dry lipid were dissolved in 5 mL of FACT at 25 °C to produce mixtures in which peptide represented 6 mol % relative to phospholipid. Solvent was then rapidly removed under reduced pressure at 45 °C on a rotary evaporator to leave thin films in 50 mL round-bottom flasks. These were subsequently placed under high vacuum for 18 h at 25 °C with continuous evacuation. Hydration was with 30 mM HEPES containing 20 mM NaCl and 5 mM EDTA, pH 7.1−7.3, made up in deuterium-depleted water. Repeated freeze-drying was often used to ensure solvent and HOD removal. Oriented samples were prepared by dissolving lipid plus peptide in a minimal volume of FACT, spotting in the center of 8 mm glass disks (Marienfeld GmbH), and air-drying to leave less than 0.5 mg of total sample per plate: 200−250 disks were stacked in a 10 mm NMR tube and 50% (by weight) deuterium-depleted water added. The tubes were then capped and samples were allowed to hydrate for 48 h at 55 °C.

^{2}H NMR spectra were acquired at 76.7 MHz on a Varian Unity 500 spectrometer by use of single-tuned Doty 5 mm and 10 mm static probes with temperature regulation to ±0.1 °C. A quadrupolar echo sequence (*21*) was employed with full phase cycling and $\pi/2$ pulse width of 4−5 μs (5 mm probe) or 8−10 μs (10 mm probe). Pulse spacing was 15−20 μs and spectral width was 100 kHz. Recycle times of 100 and 500 ms were used. Typically, spectra were processed with 150−200 Hz line broadening. T_{2e} experiments were performed by acquiring spectra with interpulse delays from 15 to 200 μs, measuring peak heights in the spectra and fitting each series to an exponential decay (*23*, *24*). ^{31}P NMR spectra were recorded at 161.7 MHz with continuous ^{1}H decoupling on a Varian Infinity Plus 400 spectrometer in a static probe with 5 and 10 mm coils, with a 5 μs $\pi/4$ pulse and 5 s recycle time. Spectral simulation was carried out with the program WSolids1 (K. Eichele and R. E. Wasylishen, Dalhousie University, Halifax, Canada), running on a Pentium III computer.

RESULTS

Amino acid sequences of the ErbB-2 transmembrane peptides examined were

ErbB-2_{TM},

HHHHHHG^{648}SPLTSIVS**A**^{657}VVGILLVVVLGVVFGILI-KRRQQKIRKYTTRRSM^{691},

and

ErbB-2_{TM}Mu,

HHHHHHG^{648}SPLTSIVS**A**^{657}VEGILLVVVLGVVFGILI-KRRQQKIRKYTTRRSM^{691}

where each amino acid is symbolized by its single-letter code and the extracellular N-terminus is to the left. The putative transmembrane domain, calculated by the method of Rost et al. (*25*) on the basis of the entire sequence, is single-underlined. Double underlining indicates the predicted motif region for dimer formation (*7*). The deuteration site (methyl side chain of Ala^{657}) is shown in boldface type. Design and bacterial expression of this and related peptides have been described by us previously (*13*). ErbB-2_{TM} represents the natural sequence from Ser^{649} to Met^{691} of human ErbB-2, with glycine at position 648 in place of Ala^{648}, and a hexaHis tag at the N-terminus. The glycine substitution ensured that spectral features arise from a single site well within the stable helical portion of the transmembrane domain. We have previously shown that this substitution did not alter the spectrum arising from Ala^{657} and that the hexaHis tag did not cause artifactual peptide behavior (*13*). The lack of influence of the hexaHis tag is further indicated by spectra arising from similarly tagged and expressed ErbB-1 (described below). ErbB-2_{TM}Mu refers to a peptide with sequence identical to that of ErbB-2_{TM} but containing the Val^{659} → Glu mutation that results in a transformed cell phenotype. CD spectra of ErbB-2_{TM} and ErbB-2_{TM}Mu in POPC bilayers were consistent with the transmembrane portion being α-helical (*13*).

Figure 1 presents ^{2}H NMR spectra for ErbB-2_{TM} and ErbB-2_{TM}Mu at 6 and 1 mol % in POPC liposomes. Note that all spectra correspond to membranes held well above the −3 °C gel-to-fluid phase transition temperature of the host matrix (*26*). We reported previously (*13*) that the spectra observed at high peptide concentration (6%) in the membrane can be understood from an examination of the relationship between spectral splitting and probe nucleus behavior as follows. Elongated amphiphiles tend to undergo rapid symmetric rotation about an axis perpendicular to the plane of fluid membranes. For deuterated molecules undergoing such motion in liposomes, eq 1 relates spectral splittings ($\Delta\nu_Q$) to molecular orientation and motional characteristics. Additional details of peptide−peptide interaction and dynamics can appear as perturbations on this general framework.

$$\Delta\nu_Q = (^3/_8)(e^2Qq/h)S_{mol}|3\cos^2\Theta_i - 1| \qquad (1)$$

e^2Qq/h is the nuclear quadrupole coupling constant (165−170 kHz for a C−D bond) (*19*, *21*), S_{mol} is the molecular order parameter (assuming axially symmetric order) describing orientational fluctuations of the C−D bond relative to the bilayer normal, and Θ_i is the average orientation of each

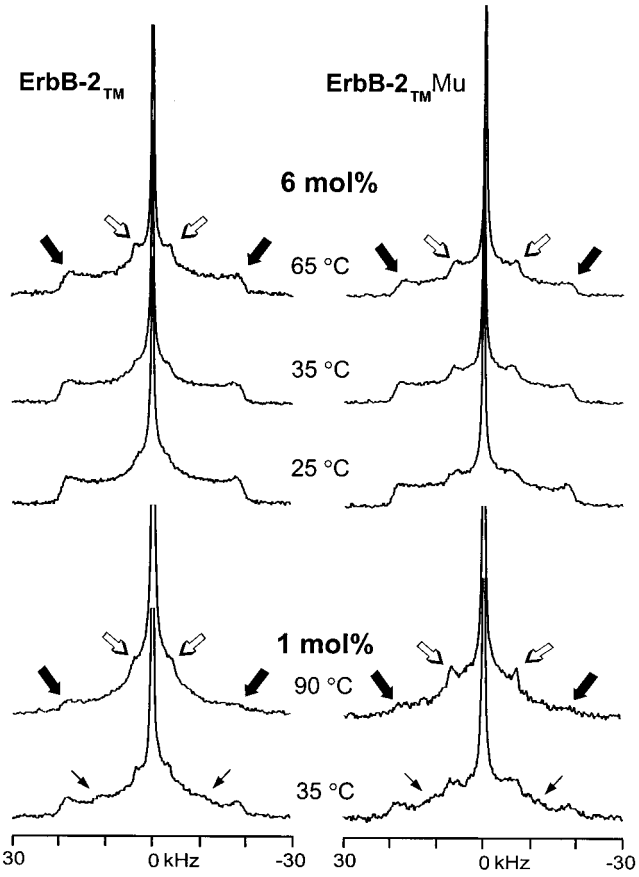

FIGURE 1: ^{2}H NMR spectra of ErbB-2 peptides at 6 and 1 mol % in POPC bilayers. Spectra are displayed for ErbB-2_{TM} (left column) and ErbB-2_{TM}Mu (right column) in fluid, fully hydrated bilayers. Peptide concentration is relative to phospholipid. Thick solid arrows indicate the 38.5 kHz splitting arising from immobilized peptide (presumed large oligomers); thick open arrows indicate narrowed Pake doublets arising from peptides whose rotational diffusion is $\gg 10^5$ s^{-1} (assigned to monomers). In the 1 mol % spectra, thin arrows indicate features attributed to dimers and/or small oligomers capable of rotation faster than 10^5 s^{-1}. Typically 500 000 transients were accumulated for 6 mol % peptide, and 1 000 000 for 1 mol %. Spectra were processed with a line broadening of 150 Hz.

C−D bond relative to the bilayer normal. For molecules having deuterated methyl groups, it is convenient to consider Θ_i to be the angle between the C−CD_3 vector and the molecular long axis and to introduce an additional factor of $^1/_3$ (the numerical value of an additional $|3\cos^2\Theta - 1|/2$ factor introduced by methyl group rapid rotation about the C−CD_3 bond where the C−C−D angle is $\Theta = 109°$). Due to the S_{mol} term in eq 1, a given splitting can be reduced under the conditions of the present experiments by wobble of the entire peptide within the membrane and by finite conformational fluctuations of the peptide backbone.

For immobilized peptides with little backbone flexibility, each alanine CD_3 group should give rise to a Pake doublet of splitting approximately 40 kHz (since rapid symmetric rotation of the methyl group about its C−CD_3 axis persists until temperatures far below 0 °C) (*15*, *27*). This spectral intensity maximum corresponds to molecules whose rotational axis happens to be at 90° to the magnetic field (statistically the most common molecular orientation in liposomes). Much lower spectral intensity extends out to twice this value for the smaller numbers of molecules having other orientations, although this is typically difficult to

distinguish from the baseline noise in unoriented-sample spectra as described later. A Pake doublet with ~40 kHz splitting arising from transmembrane peptides in fluid bilayer membranes would thus be anticipated for peptide oligomers that have been immobilized by lateral association within the membrane. Equation 1 dictates that rapid rotational diffusion of the peptide would in general lead to reduction of this splitting, to a value determined by the average orientation of the $C-CD_3$ group relative to the plane of the membrane.

Major Spectral Features of ErbB-2$_{TM}$ and ErbB-2$_{TM}$Mu at High Peptide Concentration. For ErbB-2 peptides at 6 mol % in POPC (Figure 1), a 38.5 kHz Pake doublet (thick solid arrows) is present as a major spectral component. This quadrupole splitting is very close to the ~40 kHz value expected for immobilized peptide in unoriented bilayers. Making the approximation that the membrane is a two-dimensional hexagonal array containing transmembrane peptides of diameter 10 Å, at 6 mol % peptide there would be only enough phospholipid to provide a single layer around each peptide if the latter are fully dispersed as monomers: i.e., there would be essentially only two phospholipid molecules separating nearest-neighbor peptides. Thus the spectral result seems consistent with the high peptide concentration and the fact that ErbB-2 has been suggested to have a strong tendency to lateral association. For a given sample, the 38.5 kHz Pake spectral component represents a larger fraction of overall intensity upon temperature reduction (most obvious in the 1 mol % spectra of Figure 1, described in the next section).

Each spectrum also contains an identifiable motionally narrowed Pake doublet (thick open arrows), indicating the presence of a population of peptides undergoing rotational diffusion that is fast on a time scale of $10^{-4}-10^{-5}$ s. We have previously assigned these inner peaks to ErbB-2 transmembrane peptide monomers (*13*). In the case of ErbB-2$_{TM}$ the monomer splitting is 8.2 kHz at 65 °C. Such Pake doublets, narrowed by rapid symmetric rotation, are reminiscent of spectral features that arise from alanine -CD_3 groups on end-to-end dimers of gramicidin A, which behaves as a relatively stiff transmembrane monomer rotating symmetrically in fluid bilayers (*27*, *28*). The splitting of this narrowed Pake doublet decreases slightly with temperature reduction, as discussed below. For the mutant ErbB-2$_{TM}$Mu, the monomer spectral splitting is 13.9 kHz under the same conditions. The fact that the splitting for wild-type peptide is about half that observed for the transforming mutant peptide was discussed previously (*13*): there appears to be a difference in orientation of the alanine side chain at position 657 within the motif region.

In addition to the above well-defined 38.5 kHz outer Pake doublet and the narrowed inner Pake doublet, which comprise the dominant spectral features at 6 mol % peptide, there is an intense sharp peak in the middle of each spectrum. A smaller such peak is a general feature of ^2H NMR spectra for amphiphiles in liposomes, arising from residual deuterated water and from any vesicles with high curvature, for which the quadrupole splittings are motionally averaged to zero. Central intensity buildup is also common for molecules undergoing asymmetric rotation in membranes (*20*) (i.e., rotation that occurs via 2-fold jumps or among unequally populated states). It is certainly possible that there exists a significant degree of rotational asymmetry to the motions of some fraction of the transmembrane peptides, particularly those undergoing restricted rotational diffusion.

Major Spectral Features of ErbB-2$_{TM}$ and ErbB-2$_{TM}$Mu at Lower Peptide Concentration. As peptide concentration within the membrane is reduced to 1 mol % (Figure 1, lower portion), the features attributed above to large oligomers (thick solid arrows) and to rapidly rotating monomeric peptide (thick open arrows) can still be identified. However, the relative intensity associated with the 38.5 kHz splitting is reduced in comparison to that seen at 6 mol % peptide, in keeping with the logic that this spectral feature arises from clustered peptide. With the reduced magnitude of the very broad 38.5 kHz Pake doublet at 1 mol % peptide, a new narrower doublet is apparent, having a spectral splitting of ~24 kHz in the 35 °C spectrum (thin arrows). The corresponding reduction in intensity of the Pake doublet with 38.5 kHz splitting suggests that some peptide which was previously immobilized is now rotating relatively rapidly on the NMR time scale. Appearance of new intensity in the same approximate spectral region is also apparent for the mutant peptide, ErbB-2$_{TM}$Mu, at 1 mol % and 35 °C (Figure 1, lower right-hand corner). Intensity in this region thus represents a logical candidate for the ErbB-2 transmembrane domain homodimers and higher oligomers observed as separate bands on SDS−polyacrylamide gels (*13*). Consistent with such an interpretation, as temperature is raised toward 90 °C—a temperature range in which clusters of rhodopsin transmembrane helices dissociate (reviewed in ref *16*)—these new spectral features with splittings of ~24 kHz are lost. In all cases the central unsplit peak is increased at the lower peptide concentrations: this is partly due to the presence of relatively greater amounts of residual HOD, but as noted above, central intensity is also commonly found for molecules whose rotational motion is restricted and asymmetric (*20*).

The spectral features that are suggested above to arise from rapidly rotating homodimers and/or small oligomers are more clearly resolved when peptide concentration is further lowered to 0.25 mol % (Figure 2, thin arrows). Making a hexagonal lattice approximation to phospholipid topography, at this peptide concentration there would be some 14 lipids separating neighboring fully dispersed peptides. Under these conditions, the relative intensity associated with highly immobilized molecules (thick solid arrows) has become a minor feature, and there is some sharpening of the features associated with rapidly diffusing peptide. At low temperature, where noncovalent associations might be optimal, the new splittings are well defined. In the case of the wild-type peptide (ErbB-2$_{TM}$, left-hand column), three narrowed doublets can now be assigned by examination as a function of temperature from 25 to 45 °C: the original monomer doublet (thick open arrows), plus a doublet of splitting 10−14 kHz and another of splitting 20−24 kHz (thin arrows). Peak assignment is aided by the fact that the monomer splitting (thick open arrows) decreases slightly as temperature is decreased, while the remaining narrowed splittings (assigned to homodimers and/or small oligomers) increase with temperature reduction. At 55 and 65 °C the 10−14 kHz doublet is overlapped by the monomer doublet and they are not separately resolved (this can be appreciated in the plotted spectral splittings of Figure 7 described below). Thus for ErbB-2$_{TM}$ at 65 °C in POPC, disappearance of the 38.5 kHz spectral splitting is accompanied by appearance of a distinc-

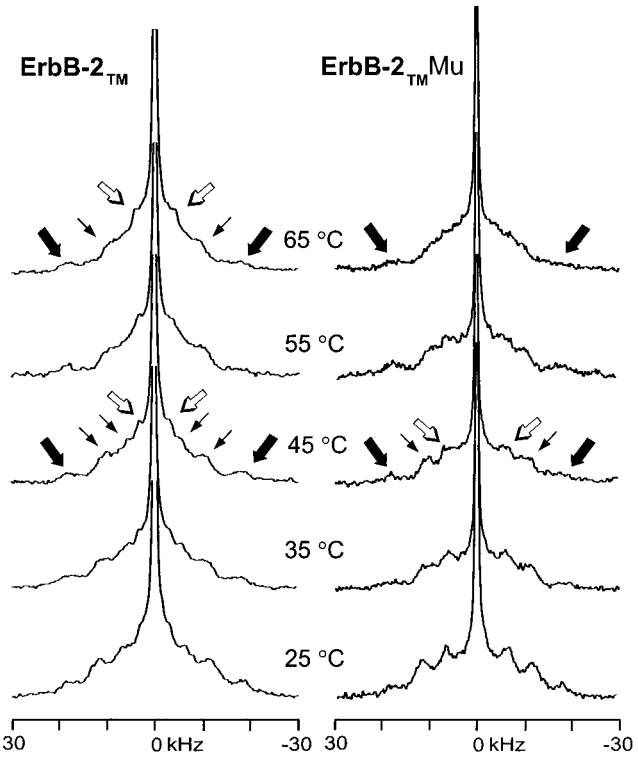

FIGURE 2: ^{2}H NMR spectra of ErbB-2 peptides at 0.25 mol % in POPC bilayers. Spectra are displayed for ErbB-2_{TM} (left column) and ErbB-2_{TM}Mu (right column) at 0.25 mol % in fluid, fully hydrated bilayers. Peptide concentration is relative to phospholipid. Thick solid arrows mark the 38.5 kHz splitting arising from immobilized peptide; thick open arrows indicate narrowed Pake doublets associated with monomeric peptide. Thin arrows refer to spectral features attributed to dimers and/or small oligomers. A total of 800 000−1 000 000 transients were accumulated, and spectra were processed with a line broadening of 150 Hz.

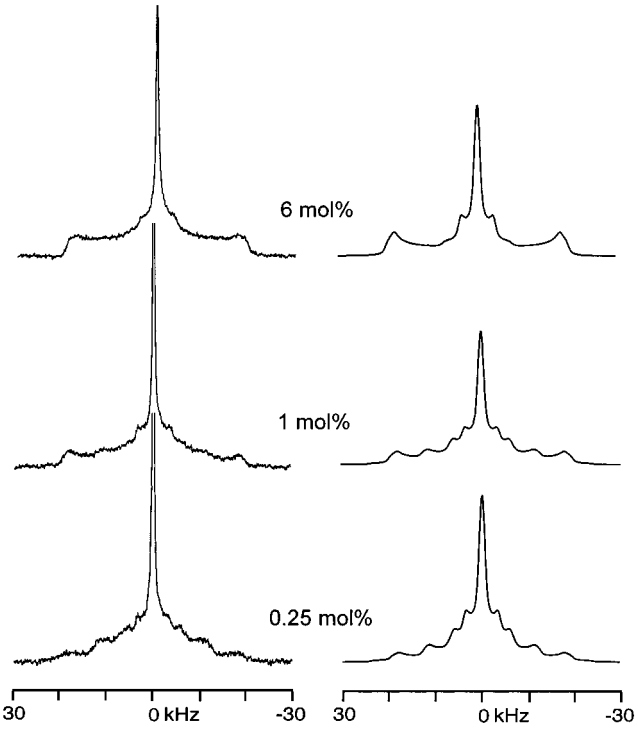

FIGURE 3: Computer simulation of ^{2}H NMR spectral line shapes. Examples of experimental spectra (left-hand column) and corresponding simulated spectra (right-hand column) are illustrated for wild-type peptides at 35 °C. Simulation was carried out by approximating each identifiable spectral splitting as a separate deuterium site of lifetime $\gg 10^{-4}$ s. These have been tentatively assigned in the manuscript to monomer, large (immobilized) oligomer, and dimer or small oligomer. An asymmetry parameter of 0.05−0.06 was applied at each site, as this proved to be necessary to fit the nonvertical outer edges of the Pake doublets. A mixed (50:50 Lorentzian:Gaussian) line-broadening function of 500−1000 Hz was applied. The center peak was simulated as a symmetric isotropic component to help match underlying central intensity but was subject to equal line broadening by the approach used.

tive doublet with splitting 20.5 kHz (thin arrows, left-hand column). As the temperature is lowered, this doublet becomes more defined and its splitting increases to 24.5 kHz, while another new doublet of splitting ∼14 kHz appears as the innermost splitting decreases.

Related phenomena are evident in spectra of ErbB-2_{TM}-Mu at 0.25% peptide (Figure 2, right-hand column). A doublet of splitting 20−24 kHz (thin arrows in the 45 °C spectrum) is clearly evident in spectra of the mutant peptide from 25 to 55 °C [with corresponding decrease of the 38.5 kHz Pake doublet seen at higher peptide concentration (thick solid arrows)]. As was the case for the wild-type peptide, the effect of temperature on the splitting of this new doublet is opposite to the effect of temperature on the feature arising from monomeric peptide (thick open arrows in the 45 °C spectrum); this effect will be discussed below surrounding Figure 7. There is some evidence that a new splitting of ∼14 kHz also occurs at low concentration in the mutant peptide as was seen in the wild type, but this region of the spectrum is obscured by the monomer peaks in the case of the mutant. It is interesting that at the (high) temperature of 65 °C, in POPC all of the mutant mobile component spectral features coalesce, while this is not as much the case for the wild type: such an effect could arise if the rates of interconversion differ, perhaps indicating that the dynamics of association are different between wild type and mutant. As noted above, in unoriented membranes all nonrotating peptides will be manifest as a common Pake doublet of splitting about 40 kHz. Hence the appearance of species having intermediate degrees of motional restriction upon reduction of peptide concentration could come about as a result of dissociation of larger microdomains into smaller ones, increased room for preexisting dimers and small oligomers to rotate rapidly, or altered lipid-mediated peptide−peptide effects.

A more quantitative assessment of spectra, including those in Figures 1 and 2, was carried out through computer simulation of the experimental spectra. This was done by assuming separate deuterium sites (in the slow exchange limit) for each identifiable spectral splitting. It proved necessary to use a nonzero asymmetry parameter (typically 0.05) in the simulations in order to match Pake doublet line shape satisfactorily. Presumably this asymmetry reflects the presence of motional and associative heterogeneity of the peptide: line broadening alone, of up to 1 kHz, did not provide a satisfactory alternative. Typical comparisons between experimental and simulated spectra are illustrated in Figure 3. In the case of 6 mol % peptide spectra (Figure 3), only two identifiable splittings existed: these splittings were assigned to immobilized oligomer and to monomer as noted above. The relative contributions of these sites required to approximate experimental spectra permitted estimation of the contributions from immobilized oligomer and monomer

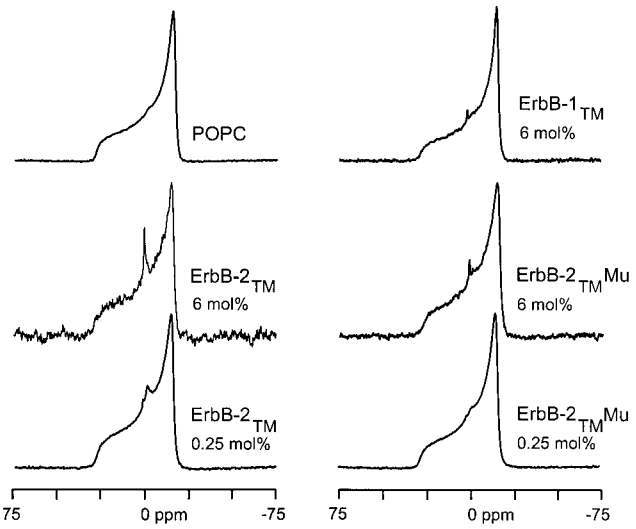

FIGURE 4: ^{31}P NMR spectra of POPC membranes containing deuterated ErbB peptides. Spectra are shown for POPC alone and for POPC containing ErbB-2_{TM} (left-hand column) and for ErbB-2_{TM}Mu (right-hand column). Examples are included for POPC containing peptide at concentrations of 6 and 0.25 mol %. All experiments were run at 35 °C. Also shown (top right) is a spectrum for POPC containing 6 mol % ErbB-1_{TM}. Spectra represent 6000−10000 accumulated transients and were processed using a line broadening of 50 Hz.

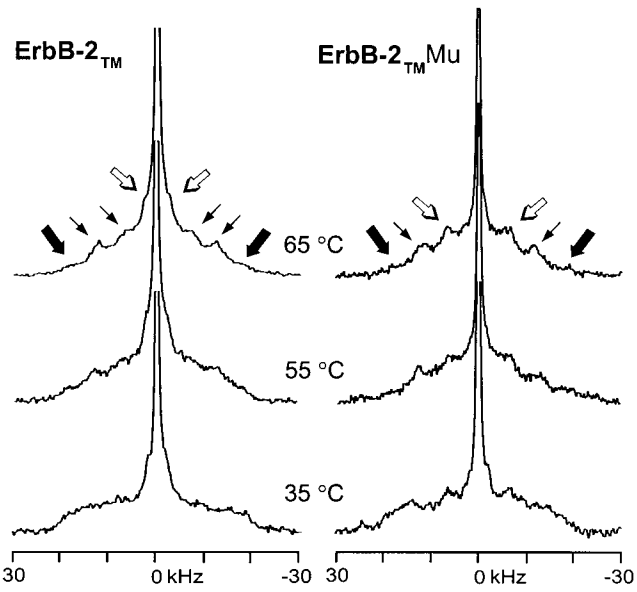

FIGURE 5: ^{2}H NMR spectra of ErbB-2 peptides in POPC/cholesterol membranes. Spectra are displayed for ErbB-2_{TM} (left column) and ErbB-2_{TM}Mu (right column) at 0.25 mol % in fluid, fully hydrated bilayers of POPC containing 33 mol % cholesterol. Thick solid arrows mark the 38.5 kHz splitting arising from immobilized peptide; thick open arrows indicate narrowed Pake doublets associated with monomeric peptide. Thin arrows indicate spectral features attributed to dimers and/or small oligomers. A total of 800 000−1 000 000 transients were accumulated, and spectra were processed with a line broadening of 150 Hz.

to be 45% and 16% ± 5%, respectively (results are displayed in Figure 3 for the wild-type peptides: within experimental error, results were comparable for the mutant peptides). Spectral simulation emphasized the fact that there was unmatched intensity of 19% associated with spectral regions immediately lateral to the monomer peak, consistent with the concept that there is underlying poorly resolved intensity associated with species rotating with intermediate rates and/or asymmetrically. A further 20% was associated with the central unsplit peak, which has been simulated for convenience as an isotropic component.

As in the case of the higher concentration samples, 1 and 0.25 mol % spectra were simulated by fitting identifiable spectral splittings as Pake doublets (examples in Figure 3, panels B and C, respectively). The presence of identifiable additional peaks (i.e., other than those assigned above to large oligomer and to monomer) at these lower concentrations made it possible to achieve a very close match to the experimental spectra. Thus at 1 mol % peptide the approximate intensities corresponded to 43% ± 5% immobile oligomer, 20% monomer, and 18% equally divided between the two Pake features assigned to dimer or small oligomer. At 0.25 mol %, the peptide spectrum was simulated by use of only 24% intensity in the large oligomer fraction, 20% monomer, and an increase to 26% intensity between the two dimer/oligomer peaks. In each case, approximately 20% could be accounted for by the central peak (which includes residual HOD and highly curved vesicles, in addition to possible contributions from asymmetric motion).

^{31}P NMR spectroscopy was employed to investigate the degree of peptide structural influence on the lipid membranes studied. The unoriented multilamellar liposome ^{2}H NMR samples described above, containing from 0 to 6 mol % peptide, were all found to produce very similar ^{31}P NMR powder patterns of width 45 ppm (Figure 4). Such patterns reflect underlying ^{31}P chemical shift anisotropy and are characteristic of phospholipids in fluid unoriented bilayer phases (ref *29* and references therein). There is typically a small spectral component at the isotropic position (0 ppm) arising from lipids that are disordered by the presence of peptide and/or by high membrane curvature. As estimated by spectral simulation and by integration, the intensity associated with this component comprised a maximum of 2.5% of the total spectrum in each case. Thus, given that some 18 lipids are required to form a single annulus around a peptide, this ^{31}P NMR component does not correlate with the magnitude of the ^{2}H NMR spectral phenomena described here or with their changes as a function of peptide concentration.

Cholesterol Effects. Figure 5shows selected spectra for ErbB-2 transmembrane peptides at 0.25 mol % in POPC bilayers containing 33 mol % cholesterol, a system intended to mimic the sterol content of cell plasma membranes. Cholesterol addition raises lipid order in fluid membranes while modestly decreasing rotational diffusion rates (*30*, *31*). Consistent with this, spectra obtained at 65 °C in the presence of cholesterol are almost superimposable (arrows in Figure 5) on those of the same samples without cholesterol at 25−35 °C (Figure 2). Additionally, as temperature is lowered, the spectral features attributed to peptide having intermediate motional restriction become typical of slowed/asymmetric motion in the cholesterol-containing membranes: broadening progressively to approach the ∼40 kHz value expected of unoriented immobilized peptide, while retaining an overall domed shape that indicates residual rotational mobility. An identifiable motionally narrowed splitting corresponding to monomeric species remains visible, demonstrating the persistence of this mobile species in the bilayer.

ErbB-1_{TM} Exhibits Primarily Monomer Spectral Features. Clearly ErbB-2_{TM} shows a considerable tendency to self-

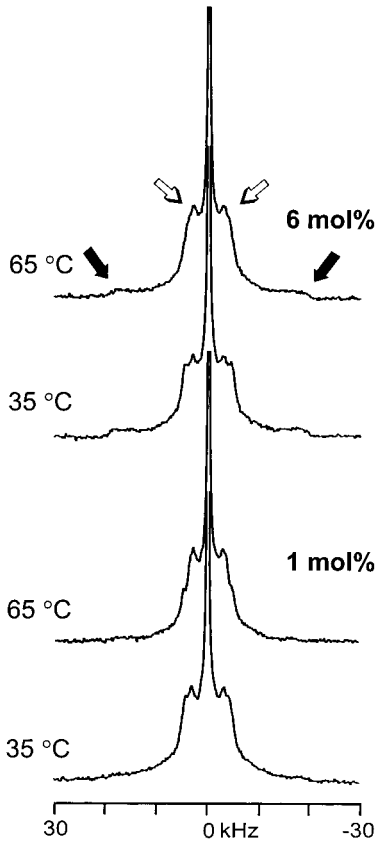

FIGURE 6: ^{2}H NMR spectra of ErbB-1_{TM} in POPC bilayers. Arrayed spectra are displayed for ErbB-1_{TM} at 6 and 1 mol %, relative to phospholipid, in fluid bilayers of POPC. Thick open arrows indicate narrowed Pake doublets associated with peptides whose rate of rotational diffusion is $\gg 10^5$ s^{-1} (assigned to monomers); thick solid arrows mark the 38.5 kHz splitting arising from peptide whose rotational rate is $\ll 10^5$ s^{-1} (assigned to large oligomers). A total of 500 000−600 000 transients were accumulated for each spectrum and processed with a line broadening of 150 Hz.

associate in fluid bilayer membranes. This fact, and the sensitivity of ^{2}H NMR to molecular orientation and dynamics, results in quite complex spectral features. We have in the past noted that synthetic transmembrane peptides from the closely related tyrosine kinase ErbB-1 (the human EGF receptor) have a predominant tendency to exist as monomers in fluid bilayers. Hence for purposes of comparison we studied a peptide, ErbB-1_{TM}, closely mimicking the transmembrane domain of ErbB-1 and produced with the same expression and isolation system described for ErbB-2_{TM} (extramembranous NH_2 terminus at left):

HHHHHHP^{620}S**I**$\underline{\mathbf{A}^{623}\text{TGVVG}\mathbf{A}^{629}}$LLLLLVV**A**^{637}LGIGLFL-RRRHIVR

ErbB-1_{TM} possesses a hexaHis tag at the same location found in the ErbB-2 peptides. As with ErbB-2_{TM}, the putative transmembrane domain and motif that might be involved in dimer formation are single- and double-underlined, respectively. Despite the presence of three deuterated alanine residues in ErbB-1_{TM} (vs only one in ErbB-2_{TM}), spectra of ErbB-2_{TM} are relatively simple because they display almost exclusively monomer features (Figure 6). The spectra consist primarily of three closely overlapping narrow Pake doublets (Figure 6, thick open arrows, spectral splittings 5−10 kHz). Similar spectral results, and spectral assignment of each alanine, have been described by us previously for synthetic transmembrane peptides from ErbB-1 (*32*). The ErbB-1_{TM} spectrum is very similar to the monomer feature described above for ErbB-2_{TM}. There is also evidence of a broader underlying component (thick solid arrows), consistent with expectations for some degree of oligomeric interaction, particularly at high peptide concentration. A ^{31}P powder spectrum for this sample is included in Figure 4, demonstrating the bilayer nature of liposomes containing ErbB-1_{TM}.

Spectra of ErbB-2_{TM} in Oriented Bilayers. The spectra described above are of randomly oriented bilayers and contain intensity contributions from all orientations of the C−D bond relative to the magnetic field of the spectrometer. Equation 1 describes the quantitative relationship for spectral contributions from those molecules whose effective C−D bond vector is at 90° to the magnetic field: i.e., this is the statistically predominant bond orientation in liposomes and hence gives rise to the intensity maxima that define each spectral doublet. The phenomenon of transmembrane peptide homodimer/homooligomer formation was further investigated in the present work by orienting the membranes containing ErbB-2_{TM} on glass plates (Figure 7). This approach to NMR of deuterated transmembrane peptides has been well developed around the bacterial species gramicidin (e.g., refs *33* and *34*) and has recently been applied to deuterated retinal in rhodopsin (*35*). Briefly, the plane of the bilayer membrane becomes parallel to that of the glass plates, which are then aligned at a chosen angle to the magnetic field. If deuterated molecules within the membrane have a preferred orientation, their ^{2}H NMR spectra can be simplified to a subset of the intensities present in their unoriented spectra. In particular, workers tend to look at alignments of the membrane parallel and perpendicular to the field. In *fluid* membranes this can have special significance: while in general the C−D bond is not directed parallel or perpendicular to the membrane long axis, rapid peptide rotation about the membrane perpendicular creates a director axis that is perpendicular to the membrane. Thus deuterated molecules rotating rapidly in the membrane display a phenomenon whereby their 90° spectral component described by eq 1 becomes more prominent upon orientation of the bilayer parallel to the field (left-hand illustration in Figure 7A). These peaks are then replaced by the 0° spectral component (at twice the splitting seen for the 90° component) when oriented with the bilayer perpendicular to the field (right-hand illustration in Figure 7A).

When POPC bilayers containing 1 mol % ErbB-2_{TM} are mechanically oriented with the magnetic field parallel to the bilayer, sharp ^{2}H NMR spectral peaks are observed at the positions noted in Figures 1 and 2 for monomeric peptide (left-hand spectrum in Figure 7A, thick open arrows, spectral splitting 8.5 kHz at 45 °C). When the sample is turned such that the field is perpendicular to the bilayer and thus along the axis of peptide rotation (right-hand spectrum), these splittings double in size to the "0° orientation" value (16.5 kHz), which was not intense enough to be seen in the unoriented spectra. It is not as clear what effect sample orientation will have on peptides rotating with intermediate rates and/or asymmetrically (but see refs *27* and *28*). However, the peaks suggested above to be associated with dimers or rapidly rotating small oligomers are present at their original positions in the left-hand spectrum of Figure 7A (thin

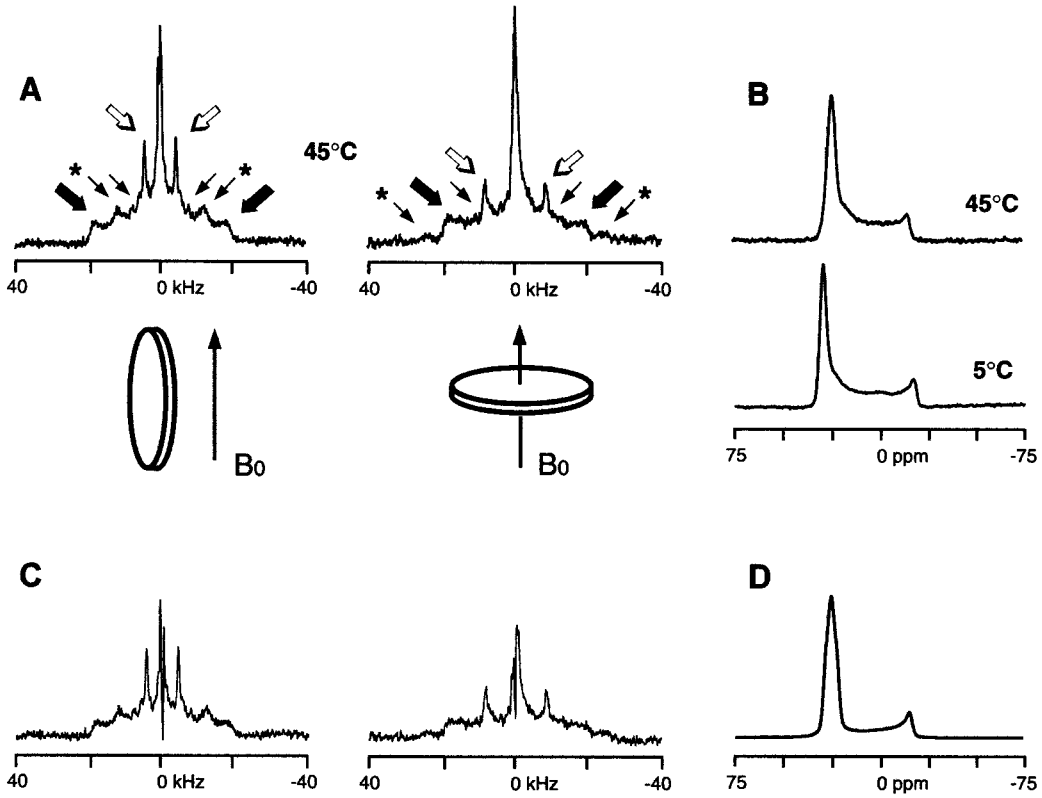

FIGURE 7: ^{2}H and ^{31}P NMR spectra of ErbB-2$_{TM}$ in uniaxially oriented bilayers. (A) ^{2}H NMR spectra for ErbB-2$_{TM}$ at 1 mol % in axially oriented, fully hydrated bilayers of POPC. Bilayers were formed on glass plates such that the plane of the membrane could be oriented parallel (left) or perpendicular (right) to the magnetic field. Below each spectrum is an illustration of membrane orientation in the field, B_0. Thick open arrows above the spectra indicate the highly narrowed spectral peaks arising from peptide whose very rapid axially symmetric rotational diffusion creates a motional director axis perpendicular to the plane of the membrane (monomeric peptide): this rapid axial rotation results in doubling of the spectral splitting when the magnetic field switches from being perpendicular to the axis of rotation (left-hand spectrum) to being along the axis of peptide rotation (right-hand spectrum). Measured splittings in the left-hand spectrum are the same as those seen in the unoriented spectra of Figures 1 and 2. Thick solid arrows indicate the 38.5 kHz splitting arising from highly immobilized peptide whose spectrum is insensitive to sample orientation. Thin arrows mark locations of spectral maxima that arise from presumed peptide dimers or small oligomers, which may undergo more restricted rotational diffusion. A total of 1 000 000 transients were accumulated. Spectra were recorded at 45 °C and processed with a line broadening of 150 Hz. (B) ^{31}P NMR spectra of mechanically aligned ErbB-2$_{TM}$ samples with the axis of peptide/lipid rotation oriented parallel to the magnetic field (as for the right-hand column in panel A above). Spectra are shown for oriented bilayers of POPC containing 1 mol % deuterated peptide and were obtained at 5 and 45 °C. Approximately 2000 transients were accumulated in each case, and spectra were processed with a line broadening of 50 Hz. (C) Effect of subtracting 30% of the powder spectrum of ErbB-2$_{TM}$ (see Figure 1) from corresponding oriented ^{2}H NMR spectra at 1 mol % peptide. This estimate of underlying powder component was obtained by spectral simulation of the ^{31}P spectral intensities in panel B, as shown in panel D.

arrows): the ~24 kHz splitting (thin arrows with asterisks) is particularly evident, while the smaller 10−14 kHz splitting (inner pair of thin arrows) is somewhat obscured by the nearby monomer peaks. Both of these features disappear from these locations upon orientation of the bilayer perpendicular to the field and reappear at twice the splitting (right-hand spectrum in Figure 7A, thin arrows). This is consistent with the interpretation that these features arise from species which are undergoing rotational diffusion in the membrane. Since the oriented samples have less water of hydration, the intensity of the sharp central peak is reduced.

Peptides rotating much slower than 10^4-10^5 s^{-1} in the oriented bilayer will not in general show a doubling of their spectral splittings upon switching bilayer orientation from parallel to perpendicular to the magnetic field (since rapid rotation is not creating a director axis perpendicular to the bilayer). Also, given that the helix axes of the peptide chains are likely tilted away from the membrane perpendicular, spectra of immobilized peptides should not be greatly affected by orientation of the membrane in the magnetic field (i.e., the C−CD$_3$ bonds will still be oriented anywhere between 0° and 90° to the field and hence will give a resultant spectral intensity mainly at 40 kHz). This seems a likely common scenario for large clusters of transmembrane peptide, consistent with the persistence of the 40 kHz peaks in all oriented spectra (Figure 7A, thick solid arrows).

It is clear from the ^{31}P NMR spectra of unoriented liposomes shown in Figure 4 that the great majority of the lipid is in bilayer form at all peptide concentrations studied. The well-aligned nature of the samples on glass plates is evident from their ^{31}P NMR spectra acquired with the magnetic field perpendicular to the membrane (Figure 7B). The dominant peak at 30 ppm is typical of phospholipid bilayers oriented perpendicular to the magnetic field, and the smaller peak at −15 ppm reflects the presence of some lipid that is orientationally or conformationally disordered by the presence of peptide as described in a systematic study of the phenomenon by Harzer and Bechinger (*36*) using model transmembrane peptides. Adopting the approach suggested by these workers (*36*), the ratio of peak intensity at 30 ppm to the sum of intensities at 30 and −15 ppm is 84%, which compares favorably to the maximum value of

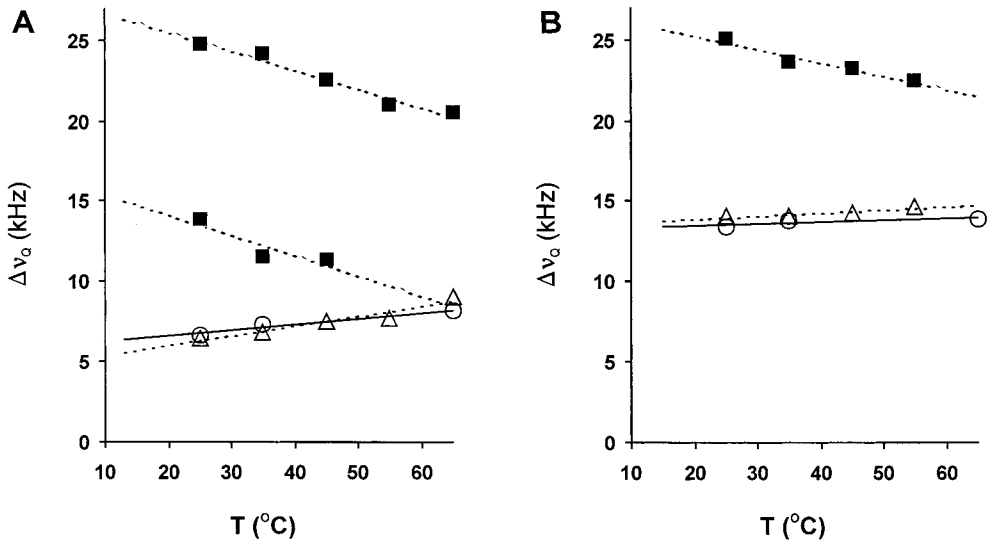

FIGURE 8: ^{2}H quadrupole splittings, $\Delta\nu_Q$, as a function of temperature for ErbB-2 peptides. Data are derived from measurements of the Ala^{657} quadrupole splitting from ErbB-2$_{TM}$ (A) and ErbB-2$_{TM}$Mu (B) in POPC bilayers. The best fit calculated via linear regression is shown for peptide incorporated at 6 mol % (solid lines) and 0.25 mol % (broken lines). Data points correspond to assigned monomer at 6 mol % (○) or 0.25 mol % (△) and to presumed dimer or rapidly rotating small oligomers (■).

90% "undisturbed lipid" reported by them for transmembrane peptides having minimal hydrophobic mismatch. Of note, there is no peak at 5 ppm where hexagonal II phase would produce a spectral maximum. Matching of the ^{31}P intensities by spectral simulation gave a lower estimate of 70% for well-oriented lipid (Figure 7D). The unoriented remaining lipid can be presumed to give rise to a predominantly powder ^{31}P spectrum. On the basis of this estimate, Figure 7C shows the result of subtracting 30% of the ^{2}H NMR spectral intensity in Figure 7A as powder spectrum (Figure 1). The effect of this subtraction is to reduce the broad underlying component, but as expected on the basis of the presumption of intermediate and slowly rotating fractions of peptide in the membrane, a major broad component remains.

Temperature Effects on ^{2}H NMR Spectral Splittings. As noted in association with Figure 1, there is a distinct difference in behavior as a function of temperature between spectral features assigned to monomer and those suggested to arise from dimers or small oligomers. These differences are apparent in graphs of spectral splitting vs temperature (Figure 8). Quadrupole splittings assigned to the rotating homodimers/homooligomers increase by 4−5 kHz with temperature reduction from 65 to 25 °C. This is a pattern typical of ^{2}H nuclei attached to a structure whose spatial arrangement is subject to thermal destabilization, as might be anticipated for dimers or small oligomers held together by (weak) noncovalent forces. The effect has its basis in the order parameter term (S_{mol}) in eq 1, which becomes larger as temperature is lowered. Quadrupole splittings assigned to the monomer are less sensitive to temperature reduction and actually decrease measurably as temperature is lowered. We have recorded the latter phenomenon previously for class I receptor tyrosine kinases (*37*, *38*) and have suggested it indicates that the helix axis is highly ordered at the temperatures studied [as noted by Koeppe et al. (*34*) and Prosser et al. (*33*) for transmembrane gramicidin]. Examination of the slopes of the lines in Figure 8 shows that the effect of temperature on the monomer spectrum is the same for 6% and 0.25% peptide in POPC.

Consideration of the Applicability of Quadrupole Echo Relaxation Times, T_{2e}. The NMR relaxation time, T_2, has the potential to be sensitive to changes in the slow motions of a molecule and might differ among molecules having different degrees of self-association. This technique was tested in the present work by recording spectra of unoriented samples as a function of interpulse spacing, τ, (Figure 9), and estimating T_2 quad echo [T_{2e} (*21*, *24*, *35*)] from semilog plots of peak heights vs time interval. The low signal-to-noise intrinsic to systems comprising low concentrations of deuterated peptides in membranes makes such experiments challenging, but it is clear from comparison of the spectra in Figure 9 that major differences in relative peak height as a function of pulse spacing were not observed. Thus large differences in T_{2e} do not exist among the peptide spectral features described above. The values determined ranged from 380 ± 100 μs for the innermost doublets to about 320 ± 100 μs for the outermost doublet. It seems likely that, while use of the -CD_3 probe makes these experiments possible by optimizing signal-to-noise ratio, it is not an ideal choice for T_2 sensitivity since methyl group rapid internal rotation becomes the dominant motional determinant.

DISCUSSION

Homodimeric interactions among receptor tyrosine kinases are considered to be major initiating events in cell signaling. Overexpression of ErbB-2, as seen in many human tumors, is often suggested to be a source of excessive interreceptor contacts and thus of tumorigenic behavior (*3*, *4*). However, it is increasingly thought that dimers may be only the minimal oligomer required for receptor activation (*39*); i.e., that higher oligomers may be equally important, or even more so, in initiating the process. Direct side-to-side interactions among the receptor transmembrane domains are claimed to provide an important mechanistic basis of dimer/oligomer formation (*10*−*12*, *40*), with van der Waals attractive forces being invoked in the context of a knobs-into-holes fit (*16*). However, measurement of the associative state of transmembrane peptides is a difficult problem. In detergent micelles,

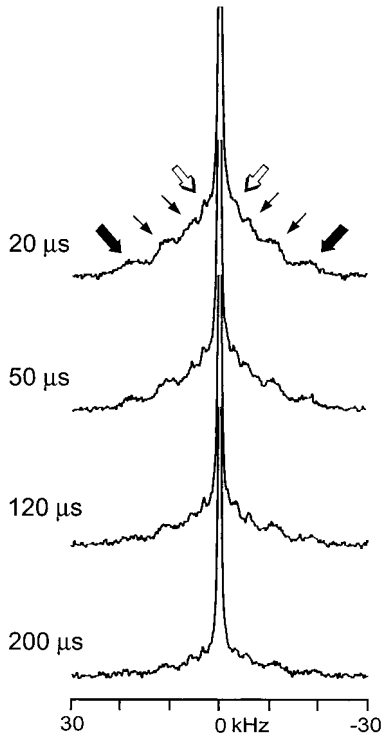

FIGURE 9: Motional effects on T_{2e} relaxation time for ErbB-2_{TM}. Spectra are arrayed for ErbB-2_{TM} at 0.25 mol % in fluid, fully hydrated bilayers of POPC at 35 °C. Interpulse delay, τ, was varied from 20 to 200 μs as indicated. Assignment of spectral features is as in Figures 1, 2, and 4: peptide large oligomers (thick solid arrows); monomeric peptide (thick open arrows); dimers and/or small oligomers (thin arrows). A total of 1 000 000 transients were accumulated, and spectra were processed with a line broadening of 150 Hz.

mixtures of apparent monomer and dimer (and sometimes higher oligomers) have been observed for transmembrane peptides from various proteins, including Neu and ErbB-2, (e.g., refs *9*, *15*, *17*, and *41*); hence monomers and dimers seem credible major species in the present NMR experiments. However, differences in the precise nature of these same peptide−peptide interactions in detergent vs lipid bilayers have been reported (*9*, *16*, *17*). Clearly this is an area of study in which a number of different approaches will supply pieces of the puzzle.

^{2}H NMR spectroscopy permits one to monitor the dynamics of molecules in fluid, fully hydrated bilayer membranes at physiological temperatures. Spectra of the deuterated peptides studied in the present work should be highly sensitive to the time-averaged orientation and motional properties of the alanine -CD_3 group, which are in turn direct reflections of the behavior and interactions of the transmembrane helix. Monomers, and small oligomers including dimers, would be expected to display significant rotational diffusion. However, the average spatial orientation of a backbone -CD_3 group would in general be measurably dependent upon whether the peptide to which it is attached is monomeric or forms part of an oligomeric unit. Moreover, the rotational motion of a small oligomer might very well be somewhat slower and less axially symmetric than that of a monomer. Very large oligomers are essentially immobile on the NMR time scale of $10^{-4}-10^{-5}$ s.

A narrowed Pake doublet, indicating the presence of rapidly rotating monomeric species, is typical of ^{2}H NMR spectra of deuterated transmembrane domains from receptor tyrosine kinases (*15*, *38*). In the present experiments this feature persisted to the highest temperatures studied (90 °C) and indeed was increased in relative intensity by heating. A broad 38.5 kHz doublet was also evident to various extents in all spectra of the expressed ErbB-2 transmembrane peptides. This feature appears justifiably associated with large oligomers whose rotational diffusion is slow relative to the NMR time scale.

Upon lowering the concentration of ErbB-2 peptides in the membrane from 6 to 1 or 0.25 mol %, new spectral features became apparent as the 38.5 kHz doublet became less dominant. Examination of these new features as a function of temperature indicated that they derive predominantly from two doublets: one having splittings of 10−14 kHz and the other 20−24 kHz over the temperature range studied. They both increased in splitting at low temperature (while the feature attributed to monomer did the opposite). It seems reasonable to suggest that these new doublets may reflect the presence of homodimers or small oligomers, whose rotational diffusion is somewhat restricted. The more obvious presence of these spectral features at low mole percentages of peptide might reflect greater ability of side-to-side dimers/small oligomers to rotate freely at low peptide concentration or increased stability of such species in a relatively undisturbed lipid matrix. In this context, it should be noted that the ^{31}P NMR experiments on the unoriented liposome samples demonstrated almost exclusively typical bilayer features and that the oriented samples did not show greater lipid headgroup disorder than expected from the degree of hydrophobic mismatch in these samples (*36*).

One might observe in passing that if both of the ^{2}H NMR doublets that are emphasized at low peptide concentration arise from dimeric peptide, the result is consistent with an asymmetric dimer (i.e., eq 1 dictates that in an asymmetric dimer the two CD_3 groups would in general have different average spatial orientations and hence different spectral splittings). Models predicting an asymmetric dimer have been developed (*7*, *12*). By the same spectral logic, the observation of distinct quadrupole splittings associated with these ^{2}H NMR features is consistent with the concept that some preferred motif or peptide−peptide binding orientation exists. The fact that one of these splittings is in the range of 20 kHz requires (eq 1) that the transmembrane helix axis be tilted some 20° or more from the membrane perpendicular (*32*), as typically proposed for dimers of class I receptor tyrosine kinases (*7*, *9*, *12*, *16*). The persistence at 65 °C of noncovalent side-to-side associations between peptides seemed somewhat surprising. However, helical transmembrane peptides are known to be remarkably stable, as a result of backbone $i \rightarrow i + 4$ hydrogen bonding. Temperatures in the range of 80 °C have been reported to be necessary to disrupt side-to-side associations between transmembrane helical domains of bacterial rhodopsin, even after the extramembranous linking portions are cleaved (reviewed in ref *16*).

While the present experiments provide clear evidence of receptor transmembrane domain association in membranes under the conditions tested, they offer limited information as to the nature of the forces involved. It is interesting that ErbB-2_{TM}Mu, containing the Val^{659}-to-Glu mutation that leads to transformed cell behavior, demonstrated spectral features similar to those of the wild-type peptide. Tradition-

ally it is suggested that the mutation leads to greater dimer formation. This may be a further reflection of negative regulatory influence by the extramembranous portions (*6*, *42*), which are largely missing in the present peptides. It is also interesting that the ErbB-1 transmembrane peptide, expressed by the same approach as the ErbB-2 species, existed primarily as monomers under the same conditions. This is consistent with observations that ErbB-2 has a particular propensity for receptor association (*43*). Note, however, that, like ErbB-2, ErbB-1 has a motif fulfilling the requirements originally suggested by Sternberg and Gullick (*7*) as a dimerization site. Clearly presence of a motif is not the only determinant of the behavior seen.

The highly immobilized large oligomers (giving rise to the 38.5 kHz spectral splitting), which were most apparent at high peptide concentration, may consist of species held together by a variety of forces. They may for instance include clusters of the homodimers envisaged by Sternberg and Gullick (*7*) and Brandt-Rauf et al. (*8*). These workers, as well as Deber, Smith, Engelman, and colleagues (*41*, *44*, *45*), have emphasized the possible significance of residues with small side chains in permitting the close side-to-side approach thought to charactize transmembrane peptide oligomers. We have proposed in past that transmembrane helical peptides might tend to associate with one another in bilayer membranes by virtue of behaving as impurities in the surrounding liquid-crystal lipid matrix and that this effect might be increased in the presence of cholesterol (*46*, *47*). Such association would not in general be expected to stop at dimer formation or necessarily to be of high affinity. These and other relevant concepts have been extensively reviewed (e.g., refs *16*, *41*, and *48*), and can be summarized in the context of a knobs-into-holes model (*16*). Thermodynamic factors involved may depend to some extent upon peptide concentration, since lipid matrix disruption by peptide may influence peptide relative orientation and intermolecular forces. Cholesterol effects seen in the present work could be readily rationalized in terms of its known matrix-ordering properties and existing models of lipid−protein interaction; however, this is a complex issue requiring consideration of alternative aspects including membrane thickness changes. Structural effects of cholesterol on transmembrane peptides in bilayer membranes have been specifically considered recently (ref *49* and references therein). It was unfortunate that T_{2e} measurements, as performed, were insensitive to the peptide motional parameters involved. One might note that Macdonald and Seelig (*50*) found that the considerably shorter T_{2e} values of ring deuterons in motionally restricted tryptophan residues on gramicidin dropped by a factor of 3 upon passing through the fluid/gel phase transition of the host lipid matrix, although the end-point values (i.e., in fluid vs gel phase membranes) were similar to one another since T_{2e} passed through a minimum at the transition.

CONCLUSIONS

Solid-state ^{2}H NMR spectroscopy of transmembrane peptides from ErbB-2 demonstrated the presence of long-lived peptide−peptide associations in lipid bilayers having key characteristics of cell membranes. At high peptide concentration, predominant spectral features could be assigned to rapidly rotating monomers and to large oligomers that were immobilized relative to a time scale of 10^{-4}−10^{-5} s. At lower peptide concentration the immobile oligomer fraction was greatly reduced, and features suggesting a rotationally mobile homodimer and/or small-oligomer population became identifiable. This work demonstrates that it is possible to separately monitor coexisting populations of transmembrane peptides whose associations are thought to modulate signaling. It also directly demonstrates the strong tendency toward stable self-association of transmembrane domains of ErbB-2. Under the conditions studied, there was no major difference in self-association between wild type and an oncogenic mutant, suggesting a modulatory role for the extramembranous portions. Results were consistent with the theory that overexpression of ErbB-2 can lead to considerable populations of interacting receptors and resultant constitutive activation. ErbB-2 has no known ligand and is thought to depend for its signaling role upon side-to-side interaction with other single-span transmembrane proteins. Thus its ready formation of associated species in the present work, and the apparent lesser degree of association of ErbB-1, may reflect an underlying natural tendency in the full-length receptor. Our findings reinforce the concept that reversible homooligomer formation among receptor transmembrane domains is an important thermodynamic consideration.

REFERENCES

1. van der Geer, P., Hunter, T., and Lindberg, R. A. (1994) *Annu. Rev. Cell Biol. 10*, 251−337.
2. Kavanaugh, W. M., and Williams, L. T. (1996) in *Signal transduction* (Heldin, C.-H., and Purton, M., Eds.) Chapman & Hall, London.
3. Hynes, N. E., and Stern, D. F. (1994) *Biochim. Biophys. Acta 1198*, 165−184.
4. Gullick, J., and Srinivasan, R. (1998) *Breast Cancer Res. Treatment 52*, 43−53.
5. Heldin, C.-H. (1995) *Cell 80*, 213−223.
6. Hubbard, S. R. (1999) *Prog. Biophys. Mol. Biol. 71*, 343−358.
7. Sternberg, M. J. E., and Gullick, W. J. (1990) *Protein Eng. 3*, 245−248.
8. Brandt-Rauf, P. W., Rackovsky, S., and Pincus, M. R. (1990) *Proc. Natl. Acad. Sci. U.S.A. 87*, 8660−8664.
9. Li, S.-C., Deber, C. M., and Shoelson, S. E. (1994) in *Peptides: Chemistry, Structure and Biology* (Hodges, R. S., and Smith, J. A., Eds.) ESCOM, Leiden, The Netherlands.
10. Brandt-Rauf, P. W., Pincus, M. R., and Monaco, R. (1995) *J. Protein Chem. 14*, 33−40.
11. Smith, S. O., Smith, C. S., and Bormann, B. J. (1996) *Nat. Struct. Biol. 3*, 252−258.
12. Sajot, N., Garnier, N., and Genest, M. (1999) *Theor. Chim. Acta 101*, 67−72.
13. Sharpe, S., Barber, K. R., and Grant, C. W. M. (2000) *Biochemistry 39*, 6572−6580.
14. Bowie, J. U. (2000) *Nat. Struct. Biol. 7*, 91−94.
15. Jones, D. H., Ball, E. H., Sharpe, S., Barber, K. R., and Grant, C. W. M. (2000) *Biochemistry 39*, 1870−1878.
16. White, S. H., and Wimley, W. C. (1999) *Annu. Rev. Biophys. Biomol. Struct. 28*, 319−365.
17. Choma, C., Gratkowski, H., and DeGrado, W. F. (2000) *Nat. Struct. Biol. 7*, 161−166.
18. Subczynski, W. K., Lewis, R. N. A. H., McElhaney, R. N., Hodges, R. S., Hyde, J. S., and Kusumi, A. (1998) *Biochemistry 37*, 3156−3164.
19. Seelig, J. (1977) *Q. Rev. Biophys. 10*, 353−418.
20. Opella, S. J. (1986) *Methods Enzymol. 131*, 327−361.
21. Davis, J. H. (1991) in *Isotopes in the Physical and Biomedical Sciences* (Buncel, E., and Jones, J. R., Eds.) Vol. 2, Elsevier, Amsterdam.
22. Siminovitch, D. J. (1998) *Biochem. Cell Biol. 76*, 411−422.

23. Bloom, M., and Sternin, E. (1987) *Biochemistry 26*, 2101−2105.
24. Köchy, T., and Bayerl, T. M. (1993) *Phys. Rev. E 47*, 2109−2116.
25. Rost, B., Fariselli, P., and Casadio, R. (1996) *Protein Sci. 5*, 1704−1718.
26. Davis, P. J., and Keough, K. M. W. (1985) *Biophys. J. 48*, 915−918.
27. Lee, K. C., Huo, S., and Cross, T. A. (1995) *Biochemistry 34*, 857−867.
28. Jude, A. R., Greathouse, D. V., Leister, M. C., and Koeppe, R. E., II (1999) *Biophys. J. 77*, 1927−1935.
29. Scherer, P. G., and Seelig, J. (1989) *Biochemistry 28*, 7720−7728.
30. Davis, J. H. (1993) in *Cholesterol in Membrane Models* (Finegold, L., Ed.) pp 67−135, CRC Press, Boca Raton, FL.
31. McMullen, T. P. W., and McElhaney, R. N. (1995) *Biochim. Biophys. Acta 1234*, 90−98.
32. Jones, D. H., Barber, K. R., VanDerLoo, E. W., and Grant, C. W. M. (1998) *Biochemistry 37*, 16780−16787.
33. Prosser, R. S., Daleman, S. I., and Davis, J. H. (1994) *Biophys. J. 66*, 1415−1428.
34. Koeppe, R. E., II, Killian, J. A., and Greathouse, D. V. (1994) *Biophys. J. 66*, 14−24.
35. Glaubitz, C., Burnett, I. J., Grobner, G., Mason, A. J., and Watts, A. (1999) *J. Am. Chem. Soc. 121*, 5787−5794.
36. Harzer, U., and Bechinger, B. (2000) *Biochemistry 39*, 13106−13114.
37. Morrow, M. R., and Grant, C. W. M. (2000) *Biophys. J. 79*, 2024−2032.
38. Sharpe, S., and Grant, C. W. M. (2000) *Biochim. Biophys. Acta 1468*, 262−272.
39. Alroy, I., and Yarden, Y. (1997) *FEBS Lett. 410*, 83−86.
40. Gullick, W. J., Bottomley, A. C., Lofts, F. J., Doak, D. G., Mulvey, D., Newman, R., Crumpton, M. J., Sternberg, M. J. E., and Campbell, I. D. (1992) *EMBO J. 11*, 43−48.
41. Lemmon, M. A., MacKenzie, K. R., Arkin, I. T., and Engelman, D. M. (1997) in *Membrane Protein Assembly* (von Heijne, G., Ed.) pp 3−23, R. G. Landes Co.
42. Rodrigues, G. A., and Park, M. (1994) *Curr. Opin. Genet. Dev. 4*, 15−24.
43. Graus-Porta, D., Beerli, R. R., Daly, J. M., and Hynes, N. E. (1997) *EMBO J. 16*, 1647−1650.
44. Javadpour, M. M., Eilers, M., Groesbeek, M., and Smith, S. O. (1999) *Biophys. J. 77*, 1609−1618.
45. Li, Z., Glibowicka, M., Joensson, C., and Deber, C. M. (1993) *J. Biol. Chem. 268*, 4584−4587.
46. Grant, C. W. M., and McConnell, H. M. (1974) *Proc. Natl. Acad. Sci. U.S.A. 71*, 4653−4657.
47. Jones, D. H., Rigby, A. C., Barber, K. R., and Grant, C. W. M. (1997) *Biochemistry 36*, 12616−12624.
48. Mouritsen, O. G., and Bloom, M. (1993) *Annu. Rev. Biophys. Biomol. Struct. 22*, 145−171.
49. Ren, J., Lew, S., Wang, J., and London, E. (1999) *Biochemistry 38*, 5905−5912.
50. MacDonald, P. M., and Seelig, J. (1988) *Biochemistry 27*, 2357−2364.

BI011340F